Anti-Tumor Effect of IDF-11774, an Inhibitor of Hypoxia-Inducible Factor-1, on Melanoma

Nan-Hyung Kim[1], Jong Heon Jeong[1], Yu Jeong Park[1], Hui Young Shin[1], Woo Kyoung Choi[1], Kyeong Lee[2] and Ai-Young Lee[1,*]

[1]*Department of Dermatology, Dongguk University Ilsan Hospital, Goyang 10326,*
[2]*BK21 FOUR Team and Integrated Research Institute for Drug Development, College of Pharmacy, Dongguk University, Goyang 10326, Republic of Korea*

Abstract

Melanoma is one of the most aggressive skin cancers. Hypoxia contributes to the aggressiveness of melanoma by promoting cancer growth and metastasis. Upregulation of cyclin D1 can promote uncontrolled cell proliferation in melanoma, whereas stimulation of cytotoxic T cell activity can inhibit it. Epithelial mesenchymal transition (EMT) plays a critical role in melanoma metastasis. Hypoxia-inducible factor-1α (HIF-1α) is a main transcriptional mediator that regulates many genes related to hypoxia. $CoCl_2$ is one of the most commonly used hypoxia-mimetic chemicals in cell culture. In this study, inhibitory effects of IDF-11774, an inhibitor of HIF-1α, on melanoma growth and metastasis were examined using cultured B16F10 mouse melanoma cells and nude mice transplanted with B16F10 melanoma cells in the presence or absence of $CoCl_2$-induced hypoxia. IDF-11774 reduced HIF-1α upregulation and cell survival, but increased cytotoxicity of cultured melanoma cells under $CoCl_2$-induced hypoxia. IDF-11774 also reduced tumor size and local invasion of B16F10 melanoma in nude mice along with HIF-1α downregulation. Expression levels of cyclin D1 in melanoma were increased by $CoCl_2$ but decreased by IDF-11774. Apoptosis of melanoma cells and infiltration of cytotoxic T cells were increased in melanoma after treatment with IDF-11774. EMT was stimulated by $CoCl_2$, but restored by IDF-11774. Overall, IDF-11774 inhibited the growth and metastasis of B16F10 melanoma via HIF-1α downregulation. The growth of B16F10 melanoma was inhibited by cyclin D1 downregulation and cytotoxic T cell stimulation. Metastasis of B16F10 melanoma was inhibited by EMT suppression.

Key Words: HIF-1α inhibitor, Inhibition of melanoma growth and metastasis, IDF11774

INTRODUCTION

Melanoma is one of the most aggressive skin cancers with high mortality, which is usually related to tumor refractoriness to conventional therapies and tumor metastasis (Schadendorf *et al*., 2018; Rebecca *et al*., 2020). Hypoxia contributes to drug resistance and tumor aggressiveness by promoting growth and metastasis of melanoma (D'Aguanno *et al*., 2021; Dratkiewicz *et al*., 2021; Singh *et al*., 2021). Drug resistance also contributes to tumor metastasis. Melanoma adapts to hypoxic conditions via upregulation of hypoxia-inducible factor-1 (HIF-1), particularly subunit α (Malekan *et al*., 2021). HIF-1α is a main transcriptional mediator that regulates many genes related to hypoxia. HIF-1α has been suggested as a biomarker

for prognosis prediction and therapeutic efficacy monitoring in melanoma based on the fact that its signalings are involved in melanoma development (Michaylira and Nakagawa, 2006; Malekan *et al*., 2021). In addition, a multicenter cohort study has suggested that expression level of intratumor HIF-1α is associated with the aggressiveness of melanoma (Martínez-García *et al*., 2017). IDF-11774 as an inhibitor of HIF-1 can inhibit HIF-1α accumulation by stimulating its degradation under hypoxic conditions in colorectal cancer cells (Ban *et al*., 2017). However, data about the role of IDF-11774 in melanoma growth and metastasis are currently unavailable.

Tumor growth is linked to cell proliferation and cell death. Cyclin D1 is a key component involved in regulation of cell cycle. Expression levels and activities of cyclin D1 are strictly

www.biomolther.org

regulated in normal cells. However, dysregulation such as up-regulation of cyclin D1 can promote uncontrolled cell proliferation, which has been identified in various cancers including melanoma (Koch *et al*., 2020; Tchakarska and Sola, 2020; González-Ruiz *et al*., 2021). In contrast, tumor cell proliferation can be inhibited by anti-tumor effect of CD8-positive T cells and their activities (Mahmoud *et al*., 2017; Pio *et al*., 2019). The role of hypoxia in immune escape has been identified (Barsoum *et al*., 2014; Li *et al*., 2018; Zou *et al*., 2018; Liu and Curran, 2020; Tittarelli *et al*., 2020; Van Duijn *et al*., 2022). For metastasis, melanoma needs to adapt to microenvironmental changes. Phenotype switching such as epithelial mesenchymal transition (EMT), which is a process acquiring mesenchymal features in epithelial cells, can be a major mechanism of melanoma metastasis, participating in key steps of metastatic cascade such as tumor migration and invasion (Pearlman *et al*., 2017; Vandyck *et al*., 2021; Nam *et al*., 2022).

This study examined the anti-cancer effect of IDF-11774, an inhibitor of HIF-1, on the growth and metastasis of melanoma. To investigate the anti-tumor effect of IDF-11774 more clearly, nude mouse model transplanted with B16F10 murine melanoma cells has been used as a transplantation animal model for such research (Shrayer *et al*., 1994; Kedinger *et al*., 2013) . Thus, both cultured B16F10 melanoma cells and nude mice transplanted with B16F10 melanoma cells were used for this study.

MATERIALS AND METHODS

Cell culture

HS936T and B16F10 melanoma cells were purchased from ATCC (Manassas, VA, USA) and Korean Cell Line Bank (Seoul, Korea), respectively. MNT1 cells were given as a gift from professor Tae-Jin Yoon (Department of Dermatology, Gyeongsang National University, Jinju, Korea). B16F10 melanoma cells were cultured in Dulbecco's modified Eagle's medium (DMEM) supplemented with 10% fetal bovine serum (FBS) and 1% penicillin/streptomycin antibiotics. For normal human melanocyte culture, individual epidermal cells prepared from circumcision adult skin specimens were suspended in Medium 254 supplemented with bovine pituitary extract, fetal bovine serum, bovine insulin, hydrocortisone, basic fibroblast growth factor, bovine transferrin, heparin, and phorbol 12-myristate 13-acetate (Invitrogen, Carlsbad, CA, USA). All cultures were maintained under standard conditions in a 5% CO_2 incubator at 37°C. For experiments, cells were cultured in each culture medium containing supplements for 24 h. These cells were then incubated with basal growth medium containing various concentrations of IDF-11774 in the presence or absence of $CoCl_2$ (Sigma-Aldrich, St Louis, MO, USA) for 48-72 h.

Melanoma formation in nude mouse model

All animal experimental protocols were approved by the Institutional Animal Care and Use Committee (IACUC) of Dongguk University Ilsan Hospital (Approval Number: 2021-04217). Twenty 4- to 6-week-old female Balb/c nude mice were subcutaneously injected with $2×10^5$ B16F10 cells suspended in 0.1 mL HEPES buffered saline to generate melanomas. When tumors grew to 100 mm^3, IDF-11774 was administered orally to four groups of mice at 0, 10, 30, and 60 mg/kg (five mice per group) for 14 days. Mice were then euthanized and tumors

were excised for measuring their volumes and immunofluorescence studies. Tumor volumes (V) were determined using the following equation: V (mm^3)=(length×width×height)×0.5.

Cell viability and cytotoxicity test

For cell viability test, cells were incubated with 3-(4,5-dimethylthiazol-2yl)-2,5-diphenyltetrazolium bromide (MTT; Sigma-Aldrich) for 4 h. Precipitated formazan was dissolved in dimethyl sulfoxide (DMSO). The optical density was measured using a spectrophotometer at 570 nm with background subtraction at 630 nm. For cytotoxicity test, lactate dehydrogenase (LDH) activity in the culture medium was measured using a cytotoxicity detection kit (Roche, Penzberg, Germany) according to the manufacturer's instructions. LDH release in supernatants of experimental cultures was determined by measuring optical density at 490 nm and then subtracting the optical density at 620 nm.

Western blot analysis

Equal amounts of extracted proteins were resolved and transferred to nitrocellulose membranes. Each membrane was incubated with one of the following antibodies: HIF-1α (mouse monoclonal; Abcam, Cambridge, UK), N-CAD, E-CAD (mouse monoclonal; Santa Cruz Biotechnology, Dallas, TX, USA), CYCLIND1, active CAS3, SNAIL (rabbit polyclonal; Cell Signaling Technology, Beverly, MA, USA), and β-Actin (mouse monoclonal; Sigma-Aldrich). After incubating with appropriate horseradish peroxidase-conjugated anti-mouse or anti-rabbit IgG antibodies (Thermo Fisher Scientific, Pittsburgh, PA, USA) and enhanced chemiluminescence solution (Thermo Fisher Scientific), signals were captured with an image reader (LAS-3000; Fuji Photo Film, Tokyo, Japan). Protein bands were then analyzed by densitometry.

Immunofluorescence staining

Biopsied skin specimens were fixed with 4% paraformaldehyde (Sigma-Aldrich) at room temperature for 24 h, embedded in paraffin wax, and then sectioned into 4-μm thick samples. After deparaffinization and rehydration, samples were preincubated with 3% bovine serum albumin. Cultured cells were fixed with 2% paraformaldehyde at room temperature for 20 min. Tissue samples or fixed cells were reacted with anti-HIF-1α, CD8, N-CAD, or SNAIL antibody and then incubated with Alexa Fluor-labelled goat anti-mouse IgG (488; Molecular Probes, Eugene, OR, USA) or Alexa Fluor-labelled goat anti-rabbit IgG (488; Molecular Probes). Nuclei were counterstained with Hoechst 33258 (Sigma-Aldrich). Fluorescence images were evaluated using an image analysis system (Dp Manager 2.1; Olympus Optical Co., Tokyo, Japan) and a Wright Cell Imaging Facility (WCIF) ImageJ software (http://www.uhnresearch.ca/facilities/wcif/imagej).

TUNEL assay

Cell apoptosis was analyzed with a terminal deoxynucleotidyl transferase dUTP nick end-labeling (TUNEL) assay using a Click-iT® TUNEL Alexa Fluor Imaging Assay Kit (Thermo Fisher Scientific) according to the manufacturer's instructions. Briefly, 4 μm sections of tumor masses extracted from melanoma-bearing mice in each treatment group were immersed in 0.25% Triton® X-100 phosphate-buffered saline (PBS) solution. After washing with PBS, sections were stained with terminal deoxynucleotidyl transferase reaction cocktail for 1 h at

37°C and then washed with PBS. After washing, Click-iT reaction cocktail and Hoechst 33342 were used to stain sections in the dark to label apoptotic cells. After staining, Hoechst 33342 and Alexa Fluor® 488 fluorescence were observed with a fluorescence microscope (Olympus Optical Co.). For quantitative measure of apoptosis, four random fields were photographed, and numbers of apoptotic cells and total cells were counted.

Statistical analysis

Data are presented as mean ± standard deviation (SD) from at least four independent experiments. Data were analyzed using the paired Student's t-test. Differences were considered statistically significant when p value was less than 0.05.
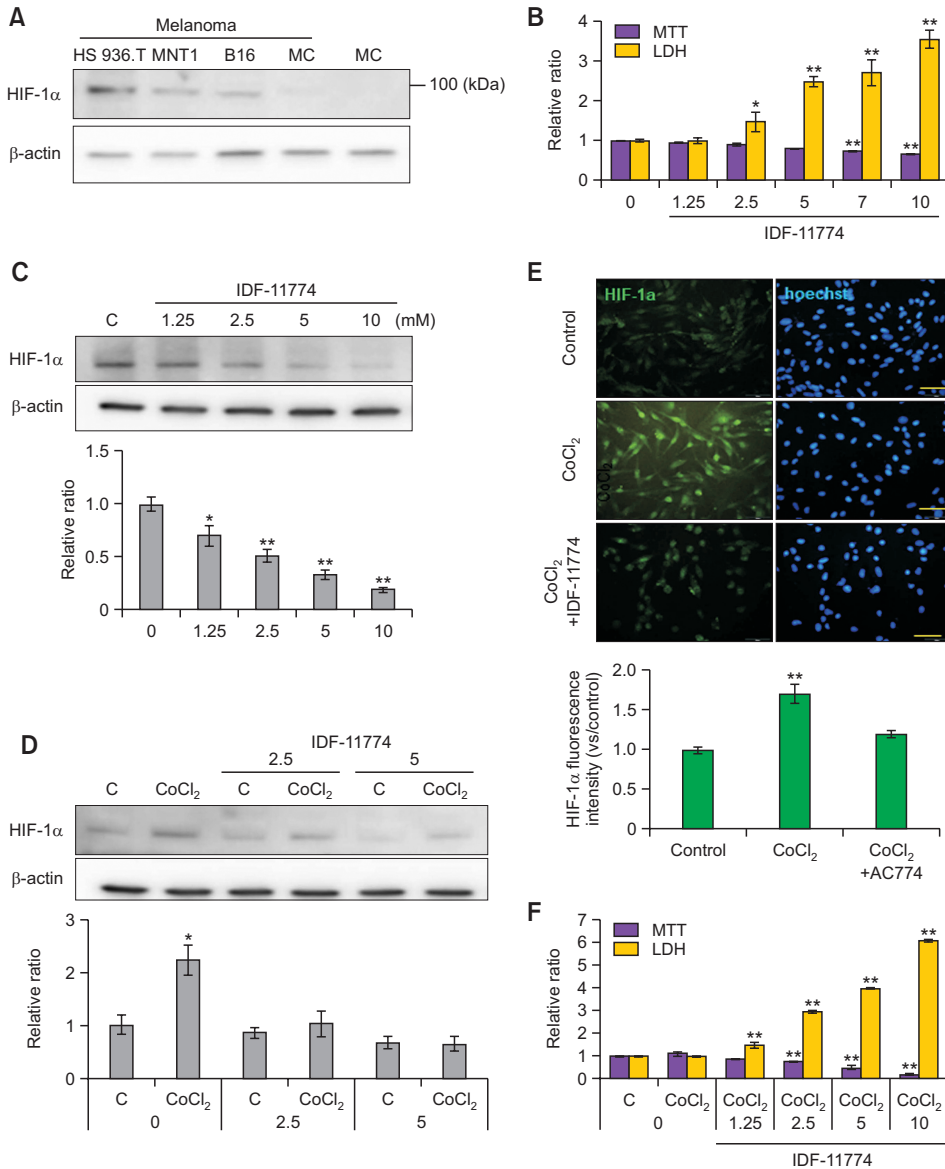
Fig. 1. IDF-11774 reduces $CoCl_2$-induced HIF-1α upregulation in cultured B16F10 melanoma cells. (A) Western blot analysis for HIF-1α protein expression in three kinds of cultured melanoma cells. (HS936T, MNT1, and B16F10) and primary cultured normal human epidermal melanocytes (MC). (B, C) MTT assay for cell viability and LDH release for cytotoxicity (B) and Western blot analysis for HIF-1α protein expression in B16F10 cells treated with different concentrations (0, 1. 25, 2.5, 5, and 10 mM) of IDF-11774 for 48 h. (D, E) Western blot analysis for relative ratios of HIF-1α levels (D) and representative immunofluorescent staining using anti-HIF-1α antibody in B16F10 treated with IDF-11774 in the absence or presence of $CoCl_2$ for 48 h. Nuclei were counter-stained with Hoechst 33258 (Bar=0.05 mm) (E). (F) MTT assay and LDH release in B16F10 treated with IDF-11774 in the absence or presence of $CoCl_2$ for 48 h. β-Actin was used as an internal control for Western blot analysis. Intensities of immunofluorescence staining were measured using a Wright Cell Imaging Facility ImageJ software. Data in the graph represent mean ± SD of relative values compared to non-treated control from four independent experiments. *p<0.05, **p<0.01.

RESULTS

IDF-11774 reduces CoCl₂-induced HIF-1α upregulation in cultured B16F10 melanoma cells

Constitutional expression levels of HIF-1α protein in three kinds of melanoma cell lines and epidermal melanocytes from two different healthy individuals were examined. B16F10 melanoma cells expressed HIF-1α protein as other human melanoma cell lines, such as HS936T and MNT1 (Fig. 1A). On the other hand, there was negligible levels of HIF-1α protein expression in primary cultured normal human melanocytes (Fig. 1A). To estimate appropriate concentrations of IDF-11774 for this study, cell viability and cytotoxicity were examined using B16F10 melanoma cells treated with different concentrations of IDF-11774. MTT assay suggested that survival of B16F10 melanoma cells was reduced by IDF-11774 in a dose-dependent manner despite a significant reduction of survival by IDF-11774 at high concentrations of 7 mM and 10 mM (Fig. 1B). LDH assay showed that IDF-11774 had a significant cytotoxic effect at concentrations higher than 2.5 mM (Fig. 1B). Expression of HIF-1α protein was reduced by IDF-11774 in a dose-dependent manner (Fig. 1C). Based on these results, IDF-11774 concentrations of 2.5 mM and 5.0 mM were chosen for the following experiments. CoCl₂ is one of the most commonly used hypoxia-mimic chemicals in cell culture (Muñoz-Sánchez and Chánez-Cárdenas, 2019; Nowak-Stępniowska *et al*., 2022). Therefore, hypoxic condition was prepared using CoCl₂ in the present study. Western blot analysis showed that expression levels of HIF-1α were significantly increased by CoCl₂. However, they were reduced by IDF-11774 treatment (Fig. 1D). Immunofluorescence staining also displayed that stronger staining intensities against anti-HIF-1α antibody induced by CoCl₂ were restored by IDF-11774 in B16F10 melanoma cells (Fig. 1E). IDF-11774 decreased melanoma cell survival, but increased their cytotoxicity at lower concentrations in the presence of CoCl₂-induced hypoxia than those in the absence of CoCl₂-induced hypoxia (Fig. 1F).

IDF-11774 decreases size and local invasion of B16F10 melanoma in nude mice along with HIF-1α downregulation

IDF-11774 increased cytotoxicity but reduced cell survival and HIF-1α expression in cultured B16F10 melanoma cells (Fig. 1D-1F). Therefore, the anti-tumor effect of IDF-11774 was examined in a B16F10 melanoma-bearing animal model. Sizes of tumor masses in B16F10 melanoma-bearing nude mice, which were measured for two weeks, were decreased by IDF-11774 in a dose-dependent manner (Fig. 2A). Light microscopy after staining with hematoxylin and eosin (H&E) suggested that tumor was not circumscribed, but infiltrated neighboring tissues in untreated control melanoma, whereas it was circumscribed with numerous empty spaces in melanoma treated with IDF-11774 (Fig. 2B). Immunofluorescence staining showed much weaker staining intensities against anti-HIF-1α antibody after treatment with IDF-11774 (Fig. 2C).
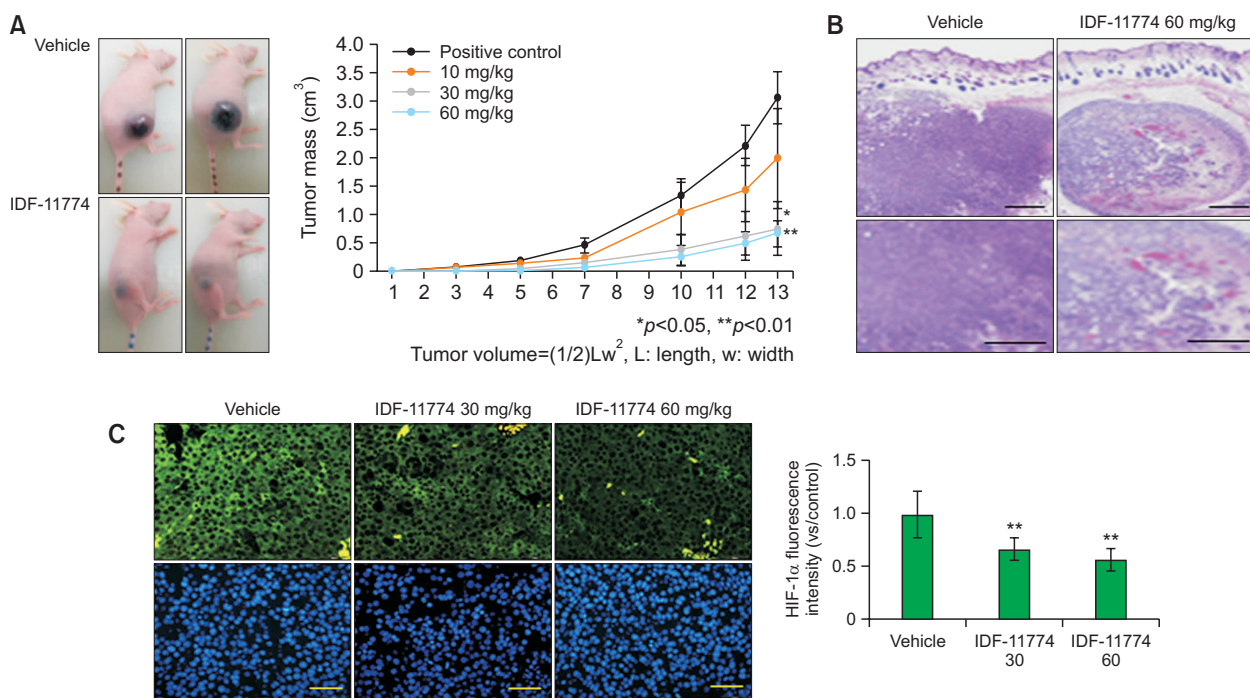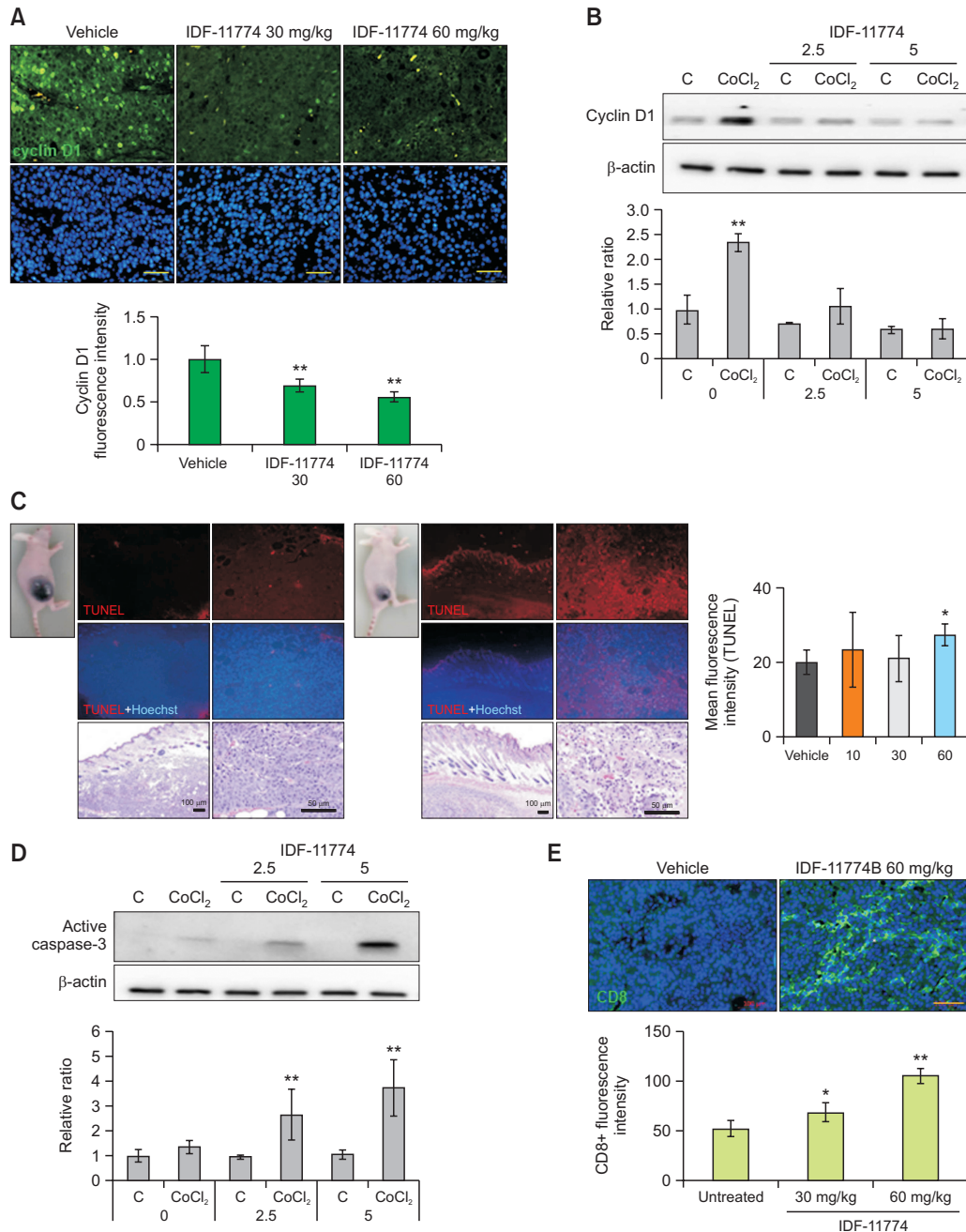

Fig. 2. IDF-11774 decreases size and local invasion of B16F10 melanoma in nude mice along with HIF-1α downregulation. (A) B16F10 melanoma in nude mice treated without (control) or with 60 mg/kg/day of IDF-11774. Data in the graph represent mean ± SD of relative melanoma volumes of mice treated with different doses of IDF-11774 compared to non-treated control, which were measured once every two or three days in five mice of each group. (B, C) Light microscopy after H&E staining (B) and representative immunofluorescent staining using anti-HIF-1α antibody (C) of B16F10 melanoma in nude mice treated without (control) or with 60 mg/kg/day of IDF-11774. Intensities of immunofluorescence staining were measured using a Wright Cell Imaging Facility ImageJ software. Nuclei were counter-stained with Hoechst 33258 (Bar=0.05 mm). Data in the graph represent mean ± SD of relative values compared to non-treated control from four independent experiments. *$p<0.05$, **$p<0.01$.

IDF-11774 decreases cyclin D1 expression but increases apoptosis and cytotoxic T-cell infiltration in B16F10 melanoma

To examine the mechanism involved in the reduction of tumor size by IDF-11774 (Fig. 2A), the role of IDF-11774 in proliferation and apoptosis of B16F10 melanoma cells was examined using cultured cells and an animal model. Immunofluorescence staining using anti-cyclin D1 antibody showed

Fig. 3. IDF-11774 decreases cyclin D1 expression but increases apoptosis and cytotoxic T-cell infiltration in B16F10 melanoma. (A) Representative immunofluorescent staining of B16F10 melanoma in nude mice treated without (control) or with 60 mg/kg/day of IDF-11774 using anti-cyclin D1 antibody. (B) Western blot analysis for relative ratios of cyclin D1 levels in cultured B16F10 treated with IDF-11774 in the absence or presence of $CoCl_2$ for 48 h. (C) Representative TUNEL assay of B16F10 melanoma in nude mice treated without (control) or with 60 mg/kg/day of IDF-11774. (D) Western blot analysis for relative ratios of active caspase-3 levels in cultured B16F10 treated with IDF-11774 in the absence or presence of $CoCl_2$ for 48 h. (E) Representative immunofluorescent staining of B16F10 melanoma in nude mice treated without (control) or with 60 mg/kg/day of IDF-11774 using anti-CD8 antibody. β-Actin was used as an internal control for Western blot analysis. Nuclei were counter-stained with Hoechst 33258 (Bar=0.05 mm). Intensities of immunofluorescence staining were measured using Wright Cell Imaging Facility ImageJ software. Data in the graph represent mean ± SD of relative values compared to non-treated control from four independent experiments. *$p<0.05$, **$p< 0.01$.
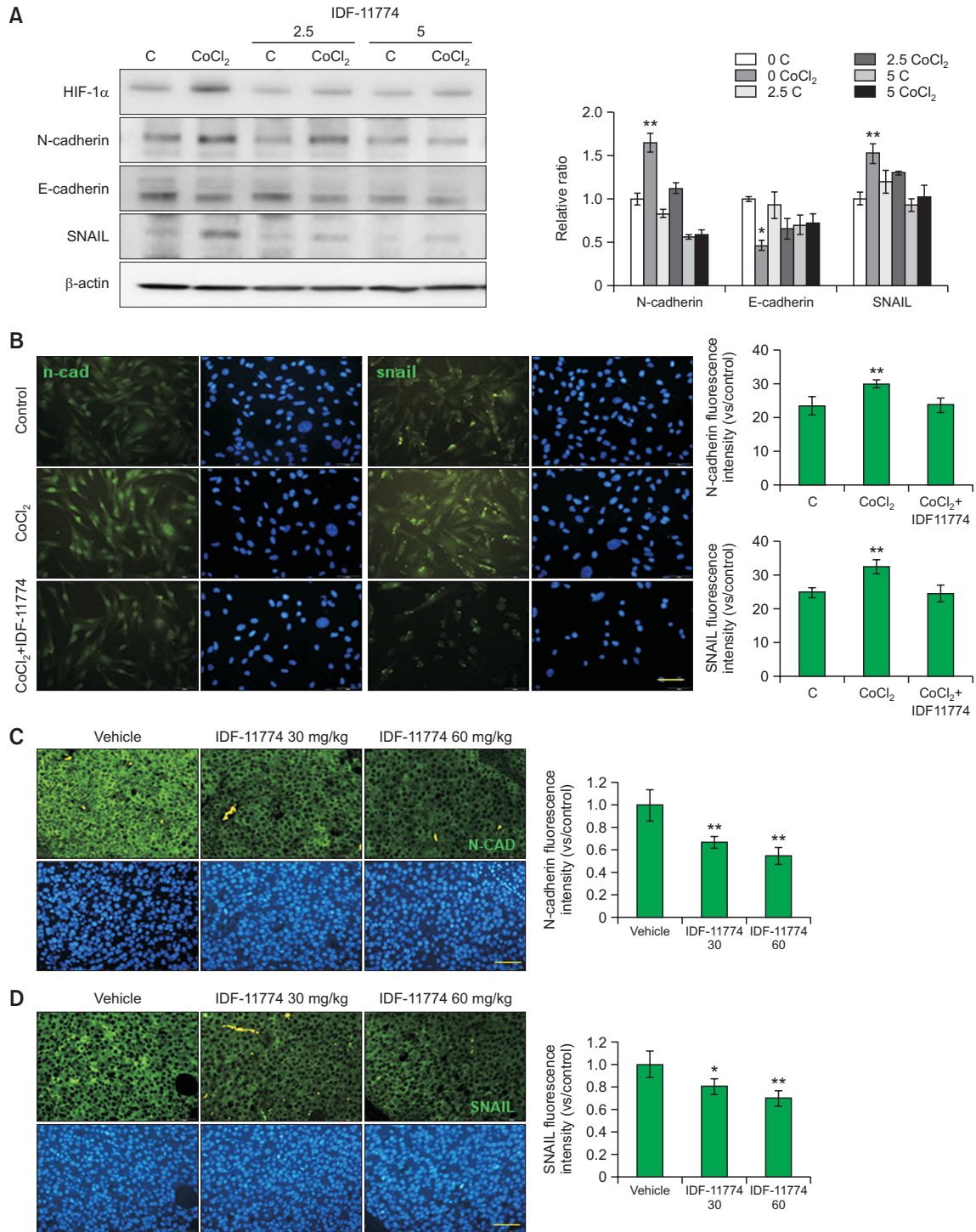
Fig. 4. IDF-11774 downregulates EMT in B16F10 melanoma. (A, B) Western blot analysis of E-cadherin, N-cadherin and SNAIL levels (A) and representative immunofluorescent staining using anti-N-cadherin or anti-SNAIL antibody (B) in cultured B16F10 treated with IDF-11774 in the absence or presence of $CoCl_2$ for 48 h. (C, D) Representative immunofluorescent staining of B16F10 melanoma in nude mice treated without (control) or with 60 mg/kg/day of IDF-11774 using anti-N-cadherin (C) or anti-SNAIL antibody (D). β-Actin was used as an internal control for Western blot analysis. Nuclei were counter-stained with Hoechst 33258 (Bar=0.05 mm). Intensities of immunofluorescence staining were measured using a Wright Cell Imaging Facility ImageJ software. Data in the graph represent mean ± SD of relative values compared to non-treated control from four independent experiments. *$p<0.05$, **$p<0.01$.

weaker staining intensities in IDF-11774-treated melanoma than in untreated melanoma (Fig. 3A). Repression of cyclin D1 expression by IDF-11774 was also shown in cultured B16F10 melanoma cells, which was increased by CoCl$_2$, in a dose-dependent manner (Fig. 3B). In contrast, the number of TUNEL-positive cells was increased in IDF-11774-treated melanoma (Fig. 3C). Levels of active caspase-3 were increased by CoCl$_2$. They were also increased in cultured B16F10 by IDF-11774 in a dose-dependent manner (Fig. 3D). Immunofluorescence staining using anti-CD8 antibody suggested stronger staining intensities in IDF-11774-treated melanoma than in untreated melanoma (Fig. 3E).

IDF-11774 downregulates EMT in B16F10 melanoma

H&E staining of untreated B16F10 melanoma suggested local invasion of tumor cells (Fig. 2B). Invasion is considered as one of the key steps of cancer metastatic cascade (Vandyck *et al*., 2021). EMT has been regarded as a major event for metastasis (Pearlman *et al*., 2017; Vandyck *et al*., 2021; Nam *et al*., 2022). Therefore, the effect of IDF-11774 on expression of E-cadherin, N-cadherin, and SNAIL was examined. Western blot analysis showed that expression levels of N-cadherin and SNAIL proteins were increased, whereas those of E-cadherin were decreased by CoCl$_2$. However, IDF-11774 restored expression levels of these proteins changed by CoCl$_2$ (Fig. 4A). Immunofluorescence staining using anti-N-cadherin and SNAIL antibodies suggested similar changes in cultured B16F10 melanoma cells (Fig. 4B). Expression levels of N-cadherin and SNAIL were lower in IDF-11774-treated melanoma than in untreated melanoma (Fig. 4C, 4D).

DISCUSSION

Expression of HIF-1α was detected in all three melanoma cell lines examined in this study, either mouse (B16F10) or human (Hs936T and MNT1) origin. HIF-1α expression levels were much lower in normal human melanocytes (Fig. 1A). HIF-1α is a main transcriptional mediator in tissue hypoxia (Malekan *et al*., 2021). Higher constitutive expression of HIF-1α in melanoma cells suggests that melanoma cells can adapt to hypoxic conditions better than normal melanocytes. Hypoxic conditions can be prepared by decreasing oxygen concentrations in cell culture using hypoxia chambers and incubators. However, due to access difficulty to such equipment in many laboratories, hypoxia-mimetic agents have been used as alternative models. CoCl$_2$ is one of the most commonly used hypoxia-mimetic chemicals in cell culture (Muñoz-Sánchez and Chánez-Cárdenas, 2019; Nowak-Stępniowska *et al*., 2022). Upregulation of HIF-1α in B16F10 melanoma cells induced by CoCl$_2$ (Fig. 1D, 1E) indicates the remarkable adaptability of B16F10 melanoma cells to hypoxia. IDF-11774 decreased the survival but increased cytotoxicity of melanoma cells with or without CoCl$_2$-induced hypoxic conditions (Fig. 1B, 1F). Because IDF-11774 reduced HIF-1α levels under the same conditions (Fig. 1C-1E), IDF-11774 might play a role in decreasing cell survival via HIF-1α downregulation. These *in vitro* effects of IDF-11774 on cell survival and cytotoxicity were also found in nude mice inoculated with B16F10 mouse melanoma cells. Oral administration of IDF-11774 recued the size

of tumor mass and HIF-1α expression levels in nude mice in a dose-dependent manner (Fig. 2A, 2C).

Significant increases of cyclin D1 expression levels were paralleled with increased expression of HIF-1α in CoCl$_2$-treated B16F10 melanoma cells (Fig. 3B). These results suggest that uncontrolled melanoma cell proliferation induced by cyclin D1 (Koch *et al*., 2020; González-Ruiz *et al*., 2021) can occur under hypoxic condition via HIF-1α. Correlation between cyclin D1 and HIF-1α target genes in melanoma (Koch *et al*., 2020) supports this result. Downregulated expression levels of CoCl$_2$-upregulated cyclin D1 by IDF-11774 (Fig. 3A, 3B) also suggests an inhibitory effect of IDF-11774 on melanoma cell proliferation via cyclin D1 inhibition as a possible mechanism for its anti-tumor effect.

In addition, increased (despite not significant) number of TUNEL-positive cells (Fig. 3C) and increased expression levels of active caspase 3 (Fig. 3D) indicate stimulatory role of IDF-11774 in apoptosis of B16F10 melanoma cells. Tumor antigen-specific cytotoxic T cells play important role in cell apoptosis (Mahmoud *et al*., 2017; Pio *et al*., 2019). Immune escape from cytotoxic T cells is essential for survival and proliferation of melanoma cells. It is known that hypoxia contributes to immune escape of cancer cells including melanoma (Barsoum *et al*., 2014; Li *et al*., 2018; Liu and Curran, 2020; Van Duijn *et al*., 2022). The tumor nest was packed with melanoma cells in untreated melanoma, whereas melanoma treated with IDF-11774 had numerous clefts and fissures (Fig. 3E). In contrast, staining intensities against CD8+ T cells were weak in untreated melanoma, whereas they were distinct in melanoma treated with IDF-11774 (Fig. 3E). These results suggest contributory role of hypoxia but an inhibitory role of IDF-11774 in immune escape of melanoma cells from cytotoxic T cells.

EMT is one of the main mechanisms for melanoma invasion and metastasis. Epithelial markers such as cytokeratins, E cadherin, and occludins are downregulated, whereas mesenchymal markers such as N-cadherin, vimentin, and fibronectin are upregulated in EMT (Kim *et al*., 2015; Pearlman *et al*., 2017; Vandyck *et al*., 2021; Nam *et al*., 2022). Decreased E-cadherin expression levels but increased N-cadherin expression in B16F10 melanoma cells under CoCl$_2$-induced hypoxic condition (Fig. 4A, 4B) indicate EMT stimulation by hypoxia. In fact, hypoxia can promote EMT in melanoma by upregulating EMT transcription factors including SNAIL (Cheli *et al*., 2012) as shown in cultured B16F10 melanoma cells under CoCl$_2$-induced hypoxia (Fig. 4A-4D). Restoration of both upregulated and downregulated above-described markers by IDF-11774 suggests an inhibitory role of IDF-11774 in metastasis of melanoma cells via suppression of EMT. Distant metastasis was not examined in two weeks after inoculating cultured B16F10 melanoma cells into nude mice. However, histopathologic findings of more circumscribed tumor boundaries in IDF-11774-administered mice compared to untreated control (Fig. 2B) might support an inhibitory effect of IDF-11774 on local invasiveness of B16F10 melanoma via EMT suppression.

In summary, IDF-11774, an inhibitor of HIF-1, can inhibit the growth and metastasis of B16F10 melanoma via HIF-1α downregulation. The growth of B16F10 melanoma was inhibited by cyclin D1 downregulation and cytotoxic T cell stimulation. B16F10 melanoma metastasis was inhibited by EMT suppression.

ACKNOWLEDGMENTS

REFERENCES

Ban, H. S., Kim, B.-K., Lee, H., Kim, H. M., Harmalkar, D., Nam, M., Park, S.-K., Lee, K., Park, J.-T., Kim, I., Lee, K., Hwang, G. S. and Won, M. (2017) The novel hypoxia-inducible factor-1α inhibitor IDF-11774 regulates cancer metabolism, thereby suppressing tumor growth. *Cell Death Dis.* **8**, e2843.

Barsoum, I. B., Smallwood, C. A., Siemens, D. R. and Graham, C. H. (2014) A mechanism of hypoxia-mediated escape from adaptive immunity in cancer cells. *Cancer Res.* **74**, 665-674.

Cheli, Y., Giuliano, S., Fenouille, N., Allegra, M., Hofman, V., Hofman, P., Bahadoran, P., Lacour, J., Tartare-Deckert, S., Bertolotto, C. and Ballotti, R. (2012) Hypoxia and MITF control metastatic behaviour in mouse and human melanoma cells. *Oncogene* **31**, 2461-2470.

D'Aguanno, S., Mallone, F., Marenco, M., Del Bufalo, D. and Moramarco, A. (2021) Hypoxia-dependent drivers of melanoma progression. *J. Exp. Clin. Cancer Res.* **40**, 159.

Dratkiewicz, E., Simiczyjew, A., Mazurkiewicz, J., Ziętek, M., Matkowski, R. and Nowak, D. (2021) Hypoxia and extracellular acidification as drivers of melanoma progression and drug resistance. *Cells* **10**, 862.

González-Ruiz, L., González-Moles, M. Á., González-Ruiz, I., Ruiz-Ávila, I. and Ramos-García, P. (2021) Prognostic and clinicopathological significance of CCND1/cyclin D1 upregulation in melanomas: a systematic review and comprehensive meta-analysis. *Cancers* **13**, 1314.

Kedinger, V., Meulle, A., Zounib, O., Bonnet, M.-E., Gossart, J.-B., Benoit, E., Messmer, M., Shankaranarayanan, P., Behr, J.-P., Erbacher, P. and Bolcato-Bellemin, A. L. (2013) Sticky siRNAs targeting survivin and cyclin B1 exert an antitumoral effect on melanoma subcutaneous xenografts and lung metastases. *BMC Cancer* **13**, 338.

Kim, H. J., Choi, W. J. and Lee, C. H. (2015) Phosphorylation and reorganization of keratin networks: Implications for carcinogenesis and epithelial mesenchymal transition. *Biomol. Ther. (Seoul)* **23**, 301-312.

Koch, A., Ebert, E. V., Seitz, T., Dietrich, P., Berneburg, M., Bosserhoff, A. and Hellerbrand, C. (2020) Characterization of glycolysis-related gene expression in malignant melanoma. *Pathol. Res. Pract.* **216**, 152752.

Li, Y., Patel, S. P., Roszik, J. and Qin, Y. (2018) Hypoxia-driven immunosuppressive metabolites in the tumor microenvironment: new approaches for combinational immunotherapy. *Front. Immunol.* **9**, 1591.

Liu, A. and Curran, M. A. (2020) Tumor hypermetabolism confers resistance to immunotherapy. *Semin. Cancer Biol.* **65**, 155-163.

Mahmoud, F., Shields, B., Makhoul, I., Avaritt, N., Wong, H. K., Hutchins, L. F., Shalin, S. and Tackett, A. J. (2017) Immune surveillance in melanoma: from immune attack to melanoma escape and even counterattack. *Cancer Biol. Ther.* **18**, 451-469.

Malekan, M., Ebrahimzadeh, M. A. and Sheida, F. (2021) The role of Hypoxia-Inducible Factor-1alpha and its signaling in melanoma. *Biomed. Pharmacother.* **141**, 111873.

Martínez-García, M. Á., Riveiro-Falkenbach, E., Rodríguez-Peralto, J. L., Nagore, E., Martorell-Calatayud, A., Campos-Rodríguez, F., Farré, R., Hernández Blasco, L., Bañuls Roca, J., Chiner Vives, E., Sánchez-de-la-Torre, A., Abad Capa, J., Montserrat, J. M., Almendros, I., Pérez-Gil, A., Cabriada Nuño, V., Cano-Pumarega, I., Corral Peñafiel, J., Diaz Cambriles, T., Mediano, O., Dalmau Arias, J. and Gozal, D.; Spanish Sleep Network (2017) A prospective multicenter cohort study of cutaneous melanoma: clinical staging and potential associations with HIF-1α and VEGF expressions. *Melanoma Res.* **27**, 558-564.

Michaylira, C. Z. and Nakagawa, H. (2006) Hypoxic microenvironment as a cradle for melanoma development and progression. *Cancer Biol. Ther.* **5**, 476-479.

Muñoz-Sánchez, J. and Chánez-Cárdenas, M. E. (2019) The use of cobalt chloride as a chemical hypoxia model. *J. Appl. Toxicol.* **39**, 556-570.

Nam, M.-W., Kim, C.-W. and Choi, K.-C. (2022) Epithelial-mesenchymal transition-inducing factors involved in the progression of lung cancers. *Biomol. Ther. (Seoul)* **30**, 213-220.

Nowak-Stępniowska, A., Osuchowska, P. N., Fiedorowicz, H. and Trafny, E. A. (2022) Insight in hypoxia-mimetic agents as potential tools for mesenchymal stem cell priming in regenerative medicine. *Stem Cells Int.* **2022**, 8775591.

Pearlman, R. L., de Oca, M. K. M., Pal, H. C. and Afaq, F. (2017) Potential therapeutic targets of epithelial-mesenchymal transition in melanoma. *Cancer Lett.* **391**, 125-140.

Pio, R., Ajona, D., Ortiz-Espinosa, S., Mantovani, A. and Lambris, J. D. (2019) Complementing the cancer-immunity cycle. *Front. Immunol.* **10**, 774.

Rebecca, V. W., Somasundaram, R. and Herlyn, M. (2020) Pre-clinical modeling of cutaneous melanoma. *Nat. Commun.* **11**, 2858.

Schadendorf, D., van Akkooi, A. C., Berking, C., Griewank, K. G., Gutzmer, R., Hauschild, A., Stang, A., Roesch, A. and Ugurel, S. (2018) Melanoma. *Lancet* **392**, 971-984.

Shrayer, D., Bogaars, H., Gersten, D., Hearing, V., Maizel, A. and Wanebo, H. (1994) Nude mouse model to study passive humoral immunotherapy directed against B16 F10 murine melanoma. *J. Surg. Oncol.* **57**, 50-56.

Singh, M., Agarwal, S., Agarwal, V., Mall, S., Pancham, P. and Mani, S. (2021) Current theranostic approaches for metastatic cancers through hypoxia-induced exosomal packaged cargo. *Life Sci.* **286**, 120017.

Tchakarska, G. and Sola, B. (2020) The double dealing of cyclin D1. *Cell Cycle* **19**, 163-178.

Tittarelli, A., Navarrete, M., Lizana, M., Hofmann-Vega, F. and Salazar-Onfray, F. (2020) Hypoxic melanoma cells deliver microRNAs to dendritic cells and cytotoxic T lymphocytes through connexin-43 channels. *Int. J. Mol. Sci.* **21**, 7567.

Van Duijn, A., Willemsen, K. J., Van Uden, N. O., Hoyng, L., Erades, S., Koster, J., Luiten, R. M. and Bakker, W. J. (2022) A secondary role for hypoxia and HIF1 in the regulation of (IFNγ-induced) PD-L1 expression in melanoma. *Cancer Immunol. Immunother.* **71**, 529-540.

Vandyck, H. H., Hillen, L. M., Bosisio, F. M., van den Oord, J., Zur Hausen, A. and Winnepenninckx, V. (2021) Rethinking the biology of metastatic melanoma: a holistic approach. *Cancer Metastasis Rev.* **40**, 603-624.

Zou, M. Z., Liu, W. L., Li, C. X., Zheng, D. W., Zeng, J. Y., Gao, F., Ye, J. J. and Zhang, X. Z. (2018) A multifunctional biomimetic nanoplatform for relieving hypoxia to enhance chemotherapy and inhibit the PD-1/PD-L1 axis. *Small* **14**, 1801120.